

Design and Synthesis of Fluorescent Probe for Polyhistidine Tag Using Macrocyclic Nickel(II) Complex and Fluorescein Conjugate

Masayasu Taki,*[1,2] Fumiyoshi Asahi,[1] Tasuku Hirayama,[1] and Yukio Yamamoto[1]

[1]Graduate School of Human and Environmental Studies, Kyoto University, Yoshida, Sakyo-ku, Kyoto 606-8501

[2]Graduate School of Global Environmental Studies, Kyoto University, Yoshida, Sakyo-ku, Kyoto 606-8501

Received October 6, 2010; E-mail: taki@chem.mbox.media.kyoto-u.ac.jp

We report a newly designed polyhistidine tag (His-tag) targeting fluorescent probe, NiL^{O}DCF, which we synthesized based on the fluorophore displacement mechanism. A macrocyclic nickel(II) complex (NiL^{O}) was employed as a novel binding site for a His-tag motif, and we chose dichlorofluorescein (DCF) (=2′,7′-dichloro-3′,6′-dihydroxyspiro[isobenzofuran-1(3*H*),9′-(9*H*)xanthen]-3-one) as the fluorophore. A hypochromic shift of NiL^{O}DCF from the metal-unbound form (L^{O}DCF) in the absorption spectrum suggested that the phenolic oxygen atom of DCF interacted directly with the NiL^{O} complex, resulting in efficient fluorescence quenching ($\Phi = 0.084$) in a neutral aqueous solution. When a model peptide having a hexahistidine sequence (H6Y1: YHHHHHH) was added to the solution of NiL^{O}DCF, a significant fluorescence enhancement in the emission ($\Phi = 0.60$) was observed. The stoichiometry of the ternary complex between NiL^{O}DCF and H6Y1 was 1:1. The fluorescence intensity increased as the concentration of H6Y1 increased, and the dissociation constant (K_d) was determined to be $24 \pm 1\,\mu M$, consistent with that for the Ni–NTA complex and His_6-fused proteins ($K_d = 1$–$20\,\mu M$). These results indicate that macrocyclic NiL^{O} can serve as a novel binding site for the polyhistidine sequence and that NiL^{O}DCF would be applicable to a switchable fluorescent probe for such His-tagged proteins.

Fluorescent labeling of proteins has been an indispensable technique for studying protein dynamics both in vitro and in vivo.[1,2] Such studies are mostly performed by expressing fluorescent proteins (FPs) at the specific site of the target protein.[3,4] Although FPs can be easily incorporated into proteins through genetic fusion, the relatively large size of FPs (ca. 27 kDa) can sterically interfere with functions, trafficking, and locations of the original proteins.[5,6] One strategy for overcoming these problems with FPs is to utilize a pair of an artificial short peptide (tag) and a small synthetic organic fluorescent probe that has sites capable of recognizing the tag sequence.[7–9] A variety of tag–probe pairs have been developed for analyzing protein expression and protein–protein interactions, as well as for fluorescent imaging of proteins in living systems.[10–19] Among them, polyhistidine tag (His-tag) and nickel(II)–2,2′,2″-nitrilotriacetato complex (Ni–NTA) are the most well-known complementary pair and various Ni–NTA derivatives with an appended fluorophore have been developed as the probe.[20–26] However, only a few fluorescent Ni–NTA complexes, for which the labeling event can be monitored by means of a detectable fluorescent signal, have been reported.[24–26] Therefore, in most cases, removal of the non-labeled probe molecule is required to reduce the fluorescence background prior to analyzing protein dynamics and the optical imaging experiment.

Ni–NTA complexes are known to bind not only with nitrogen-containing aromatic heterocyclic compounds but also with aliphatic amines. By taking advantage of such coordinative ability of Ni–NTA complexes, Higuchi, Umezawa, et al. recently developed hydroxycoumarin-based fluorescent M–NTA (M = Co^{II} or Ni^{II}) complexes,[24,25] designed on the basis of a fluorophore displacement strategy,[27,28] which show a turn-on response in the emission upon binding to a His-tag-fused protein. In this system, fluorescence is largely quenched due to a labile interaction with a paramagnetic metal center (Co^{II} or Ni^{II}) supported by an NTA ligand. When a His-tag-fused protein is present, dissociation of the fluorophore from the coordination sphere of the metal ion occurs, increasing the strength of the fluorescence. However, the hydroxycoumarin fluorophore requires a short excitation wavelength (≈360 nm), which can cause serious damage to cells. Although fluorescein and boron–dipyrromethene (BODIPY) derivatives are the most commonly used as a visible light excitable fluorescent molecule, electron-donating ability of the amino group introduced into these fluorophores usually causes fluorescence quenching through a photoinduced electron-transfer process,[29–32] which may result in decreasing the fluorescence intensity of the fluorophore-displaced form. Anionic functional groups such as carboxylate and phenolate are other candidates for the coordinative donors to the metal ions. However, the affinities of Ni–NTA complexes for these functional groups are much weaker compared with those for aromatic and aliphatic amines.[14,17,33] Indeed, Lippard et al. have reported that fluorophore emission of the NTA–fluorescein construction remained almost unchanged upon complexation with Ni^{II},[23] indicating no interaction between the Ni–NTA complex and the anionic fluorescein dye. For all these reasons, the choice of an appropriate fluorophore is quite limited when a Ni–NTA complex is utilized as the His-tag binding site of the fluorescent probe based on the fluorophore displacement mechanism.

Published on the web April 7, 2011; doi:10.1246/bcsj.20100288

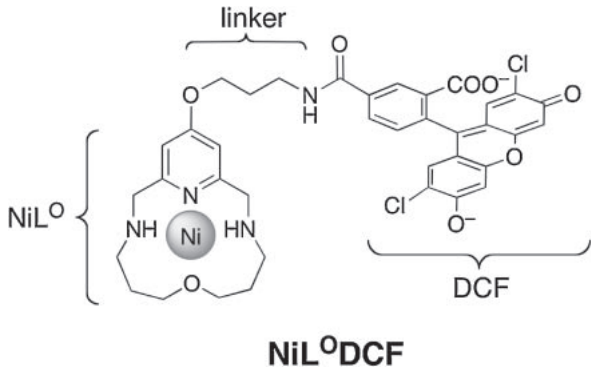

Figure 1. Structure of a designed fluorescent probe NiL^{O}DCF consisting of a macrocyclic Ni^{II} complex (NiL^O), dichlorofluorescein (DCF), and a flexible linker.

Therefore, it has been challenging to develop alternatives to Ni–NTA that can both quench the fluorescence via a labile interaction with anionic functional groups of the fluorophore and bind with the His-tag motif of proteins.[15,19]

In this paper, we report a newly designed polyhistidine tag (His-tag) targeting fluorescent probe, NiL^{O}DCF (Figure 1), which we synthesized based on the fluorophore displacement mechanism. This probe consists of two units, macrocyclic nickel(II) complex (NiL^O)[34] as a novel binding site for a His-tag motif and dichlorofluorescein (DCF) (=2′,7′-dichloro-3′,6′-dihydroxyspiro[isobenzofuran-1(3*H*),9′-(9*H*)xanthen]-3-one) as a visible light excitable fluorophore, and these components are linked by a flexible chain. We found that NiL^{O}DCF exhibits an increase in fluorescence in the presence of the His-tag and that NiL^O can act as the His-tag binding site with a comparable binding affinity to the Ni–NTA/His$_6$ pair.

Experimental

All chemicals used in this study were commercial products of the highest available purity and were further purified by standard methods, if necessary. A macrocyclic nickel complex [Ni(L^O)(CH$_3$CN)$_2$](ClO$_4$)$_2$,[34] diethyl 4-hydroxypyridine-2,6-dicarboxylate,[35] and 6-carboxy-2′,7′-dichloro-3′,6′-bis(pivaloyloxy)spiro[isobenzofuran-1(3*H*),9′-(9*H*)xanthen]-3-one,[36] were prepared according to published procedures. A model peptide of histidine-tag was synthesized by solid-phase synthesis (Fmoc-method) as previously reported.[37] NMR spectra were recorded on a JEOL JNM-EX-270 (at 270 MHz to ^{1}H, 68 MHz to ^{13}C) or a JEOL α-500 (at 500 MHz to ^{1}H, 126 MHz to ^{13}C). Chemical shifts are given in ppm relative to tetramethylsilane (TMS). Electrospray ionization mass spectra (ESI-MS) were recorded with micrOTOF II focus (Bruker Daltonics). Matrix-assisted laser desorption/ionization time-of-flight mass spectrometry (MALDI-TOF) was performed on autoflex III (Bruker Daltonics). High-resolution mass spectra (HRMS) were measured with a JMS-DX-300 (JEOL). Elemental analysis was done at the Elementary Analysis Center in the Graduate School of Pharmaceutical Science, Kyoto University. TLC analyses were performed on Silica gel 60-F254 (Merck). Flash chromatography was performed on silica gel (Merck Silica Gel 60). Reverse phase HPLC was performed on Waters Delta 600 system (10 × 250 mm^2 XBridgeTMC18).

Diethyl 4-[3-(*N*-Benzyloxycarbonyl)aminopropoxy]-2,6-pyridinedicarboxylate (1). To a solution of diethyl 4-hydroxy-2,6-pyridinedicarboxylate[35] (2.5 g, 10 mmol) in CH$_3$CN (10 mL) were added a solution of benzyl 3-bromopropylcarbamate (2.8 g, 10 mmol) in CH$_3$CN (10 mL) and K$_2$CO$_3$ (2.1 g, 0.016 mmol). The solution was refluxed overnight and the filtrate was evaporated. The residue was purified by flash chromatography (hexane–EtOAc, 1:1) to give **1** as a white solid (2.8 g, 62%). ^{1}H NMR (270 MHz, CDCl$_3$): δ 1.46 (t, 6H, J = 7.3 Hz), 2.08 (m, 2H), 3.43 (m, 2H), 4.20 (t, 2H, J = 5.9 Hz), 4.47 (q, 4H, J = 7.3 Hz), 4.92 (m, 1H), 5.10 (s, 2H), 7.30–7.40 (m, 5H), 7.77 (s, 2H). ^{13}C NMR (68 MHz, CDCl$_3$): δ 14.2, 29.1, 37.9, 62.4, 66.3, 66.8, 114.2, 128.1, 128.5, 136.3, 150.2, 156.4, 164.6, 166.6. ESI-TOF (pos.): calcd for C$_{22}$H$_{27}$N$_2$O$_7$ [M + H]$^+$ 431.2, found 431.3.

4-[3-(*N*-Benzyloxycarbonyl)aminopropoxy]-2,6-pyridinedimethanol (2). To a solution of **1** (2.2 g, 5.0 mmol) in a mixture of EtOH (10 mL) and THF (15 mL) was added NaBH$_4$ (0.84 g, 22.2 mmol) in portions over 5 min at 0 °C. After stirring for 1 h at room temperature, the reaction mixture was evaporated. The residue was dissolved in water (100 mL) and extracted with EtOAc (3 × 100 mL). The combined organic layer was dried over MgSO$_4$ and evaporated to give **2** as a white solid (1.6 g, 93%). This compound was used for the next step without further purification. ^{1}H NMR (270 MHz, CDCl$_3$): δ 2.01 (m, 2H), 3.38 (m, 2H), 4.07 (t, 2H, J = 5.8 Hz), 4.67 (s, 4H), 5.01 (brs, 1H), 5.09 (s, 2H), 6.69 (s, 2H), 7.29–7.39 (m, 5H). ^{13}C NMR (68 MHz, CDCl$_3$): δ 29.2, 38.0, 64.4, 65.6, 66.7, 105.5, 128.0, 128.1, 128.5, 136.4, 156.6, 160.7, 166.3. ESI-TOF (pos.): calcd for C$_{18}$H$_{23}$N$_2$O$_5$ [M + H]$^+$ 347.2, found 347.3.

4-[3-(*N*-Benzyloxycarbonyl)aminopropoxy]-2,6-pyridinedimethyl Ditosylate (3). A solution of tosyl chloride (1.4 g, 7.1 mmol) in THF (3 mL) was added to an ice-cooled solution of **2** (1.2 g, 3.6 mmol) in THF (5 mL), and then 5 mL of 2.4 M aqueous NaOH solution was added to the mixture. After stirring for 4 h at room temperature, the reaction mixture was evaporated. The residue was diluted with water (30 mL) and extracted with CHCl$_3$ (3 × 30 mL). The combined organic layer was dried over MgSO$_4$ and evaporated. The residue was purified by flash chromatography (hexane–EtOAc, 1:1) to give **3** as a white solid (1.8 g, 77%). ^{1}H NMR (270 MHz, CDCl$_3$): δ 2.02 (m, 2H), 2.44 (s, 6H), 3.39 (m, 2H), 4.04 (t, 2H, J = 5.6 Hz), 4.97 (s, 4H), 5.11 (s, 2H), 6.81 (s, 2H), 7.30–7.40 (m, 9H), 7.80 (d, 4H, J = 8.1 Hz). ^{13}C NMR (68 MHz, CDCl$_3$): δ 21.57, 29.06, 37.91, 65.80, 66.67, 71.06, 107.6, 128.0, 128.0, 128.1, 128.5, 129.9, 132.5, 136.4, 145.1, 155.1, 156.4, 166.4. ESI-TOF (pos.): calcd for C$_{32}$H$_{35}$N$_2$O$_9$S$_2$ [M + H]$^+$ 655.2, found 655.2.

4-[3-(*N*-Benzyloxycarbonyl)aminopropoxy]-2,6-bis(bromomethyl)pyridine (4). A solution of **3** (2.9 g, 4.4 mmol) and LiBr (3.8 g, 44 mmol) in acetone (35 mL) was refluxed for 8 h. After the reaction mixture was evaporated, the residue was dissolved in EtOAc (100 mL) and the organic layer was washed with water (3 × 100 mL), dried over MgSO$_4$, and evaporated to give the product **4** as a white solid (2.2 g, 100%). This compound was used for the next step without further purification. ^{1}H NMR (270 MHz, CDCl$_3$): δ 2.05 (m, 2H), 3.41 (m, 2H), 4.10 (t, 2H, J = 5.9 Hz), 4.47 (s, 4H), 4.93 (brs, 1H),

5.11 (s, 2H), 6.87 (s, 2H), 7.30–7.40 (m, 5H). ^{13}C NMR (68 MHz, $CDCl_3$): δ 29.2, 33.4, 38.0, 65.8, 66.7, 109.2, 128.1, 128.2, 128.5, 136.4, 156.4, 158.2, 166.3. ESI-TOF (pos.): calcd for $C_{18}H_{20}N_2O_3{}^{79}Br_1{}^{79}Br_1Na_1$ $[M + Na]^+$ 492.97, found 492.97; calcd for $C_{18}H_{20}N_2O_3{}^{79}Br_1{}^{81}Br_1Na_1$ $[M + Na]^+$ 494.97, found 494.97; calcd for $C_{18}H_{20}N_2O_3{}^{81}Br_1{}^{81}Br_1Na_1$ $[M + Na]^+$ 496.97, found 496.97.

Bis[3-(2-nitrophenylsulfonylamino)propyl] Ether (5). A solution of 2-nitrophenylsulfonyl chloride (2.06 g, 20 mmol) in THF (50 mL) was added to a solution of bis(3-aminopropyl) ether (1.03 g, 7.8 mmol) and $NaHCO_3$ (2.62 g, 31 mmol) in THF (50 mL) at 0 °C. The mixture was stirred overnight at room temperature and evaporated in vacuo. The residue was dissolved in saturated $NaHCO_3$ aqueous solution (100 mL) and extracted with CH_2Cl_2 (3 × 100 mL). The combined organic layers were dried over $MgSO_4$ and evaporated to give dinosylamide **5** as a white solid (3.98 g, 100%). The purity was sufficient for the following reaction. ^{1}H NMR (270 MHz, $CDCl_3$): δ 1.82 (m, 4H), 3.22 (m, 4H), 3.50 (t, 4H, $J = 5.5$ Hz), 5.78 (t, 2H, $J = 5.8$ Hz), 7.70–7.77 (m, 4H), 7.80 (d, 2H, $J = 9.2$ Hz), 8.14 (d, 2H, $J = 9.7$ Hz). ^{13}C NMR (68 MHz, $CDCl_3$): δ 29.1, 42.0, 69.2, 125.3, 131.0, 132.9, 133.4, 133.5, 147.9. ESI-TOF (pos.): calcd for $C_{18}H_{22}N_4O_9S_2Na_1$ $[M + Na]^+$ 525.07, found 525.15.

15-[3-(*N*-Benzyloxycarbonyl)aminopropoxy]-3,11-bis(2-nitrobenzenesulfonyl)-7-oxa-3,11,17-triazabicyclo[11.3.1]-heptadeca-1(17),13,15-triene (6). A mixture of **5** (0.97 g, 2.1 mmol) and Na_2CO_3 (1.1 g, 10 mmol) in dry DMF (80 mL) was stirred for 2 h at 100 °C under argon atmosphere. After cooling to room temperature, a solution of **4** (1.0 g, 2.0 mmol) in dry DMF (80 mL) was added dropwise to the mixture over 5 h by using a dropping funnel. After stirring overnight at room temperature, the reaction mixture was evaporated. The residue was dissolved in CH_2Cl_2 (100 mL) and washed with 0.1 M aqueous NaOH solution (3 × 100 mL). The combined organic layer was dried over $MgSO_4$ and evaporated. The crude product was purified by flash chromatography (hexane–EtOAc, 1:3) to give **6** as a white solid (0.86 g, 52%). ^{1}H NMR (270 MHz, $CDCl_3$): δ 1.67 (m, 4H), 2.00 (m, 2H), 3.21 (t, $J = 5.3$ Hz, 4H), 3.31 (t, 4H, $J = 7.3$ Hz), 3.38 (m, 2H), 4.00 (t, 2H, $J = 5.6$ Hz), 4.52 (s, 4H), 4.93 (brs, 1H), 5.12 (s, 2H), 6.90 (s, 2H), 7.26–7.38 (m, 5H), 7.63–7.72 (m, 6H), 8.06 (d, 2H, $J = 8.9$ Hz). ^{13}C NMR (68 MHz, $CDCl_3$): δ 27.8, 28.9, 37.8, 44.2, 53.3, 65.4, 66.5, 66.8, 109.3, 124.1, 128.0, 128.4, 130.4, 131.7, 132.8, 133.7, 136.4, 148.0, 156.4, 156.8, 166.5. ESI-TOF (pos.): calcd for $C_{36}H_{41}N_6O_{12}S_2$ $[M + H]^+$ 813.22, found 813.26; calcd for $C_{36}H_{40}N_6O_{12}S_2Na_1$ $[M + Na]^+$ 835.20, found 835.23.

15-(3-Aminopropoxy)-3,11-bis(2-nitrobenzenesulfonyl)-7-oxa-3,11,17-triazabicyclo[11.3.1]heptadeca-1(17),13,15-triene (7). A mixture of **6** (220 mg, 0.28 mmol) in 25% HBr–acetic acid solution (2 mL) was stirred for 1 h at room temperature. The reaction mixture was poured into Et_2O (100 mL) and the resulting precipitation was collected by filtration. The deliquescent material thus obtained was dissolved in MeOH and the solvent was again evaporated to dryness. The residue was dissolved in saturated $NaHCO_3$ solution (20 mL) and extracted with $CHCl_3$ (3 × 20 mL). The combined organic layer was dried over $MgSO_4$ and evaporated to give amine **7** as a yellow oil (190 mg, 100%). The purity was confirmed by ^{1}H NMR and compound **7** was used for the next step without further purification. ^{1}H NMR (270 MHz, $CDCl_3$): δ 1.66 (m, 4H), 1.94 (m, 2H), 2.92 (t, 2H, $J = 6.3$ Hz), 3.22 (t, 4H, $J = 5.3$ Hz), 3.32 (t, 4H, $J = 7.4$ Hz), 4.06 (t, 2H, $J = 5.9$ Hz), 4.52 (s, 4H), 6.93 (s, 2H), 7.65–7.75 (m, 6H), 8.05 (d, 2H, $J = 9.4$ Hz).

2′,7′-Dichloro-3-oxo-3′,6′-bis(pivaloyloxy)spiro[isobenzofuran-1(3*H*),9′-(9*H*)xanthene]-6-carboxylic Acid 2,5-Dioxo-1-pyrrolidinyl Ester (8). A solution of 6-carboxy-2′,7′-dichloro-3′,6′-bis(pivaloyloxy)spiro[isobenzofuran-1(3*H*),9′-(9*H*)xanthen]-3-one[36] (330 mg, 0.53 mmol), 1-ethyl-3-(3-dimethylaminopropyl)carbodiimide hydrochloride (EDC) (140 mg, 0.74 mmol), and *N*-hydroxysuccinimide (67 mg, 0.58 mmol) in dry CH_2Cl_2 (10 mL) were stirred for 4 h at room temperature under argon atmosphere in the dark. EDC (20 mg, 0.11 mmol) was further added to the reaction mixture and stirring was continued for an additional 3 h. After removal of the solvent, the residue was dissolved in EtOAc (50 mL) and the organic layer was washed with brine (3 × 50 mL), dried over $MgSO_4$, and evaporated. The residue was purified by flash chromatography ($CHCl_3$) to give **8** as a pale yellow solid (250 mg, 67%). ^{1}H NMR (270 MHz, $CDCl_3$): δ 1.40 (s, 18H), 2.90 (s, 4H), 6.85 (s, 2H), 7.17 (s, 2H), 7.91 (s, 1H), 8.22 (d, 1H, $J = 8.1$ Hz), 8.44 (d, 1H, $J = 8.1$ Hz). ESI-TOF (pos.): calcd for $C_{35}H_{30}N_1O_{11}Cl_2$ $[M + H]^+$ 710.12, found 710.12.

Compound 9. A solution of **7** (240 mg, 0.35 mmol) and **8** (260 mg, 0.36 mmol) in dry DMF (5 mL) was stirred overnight at room temperature under argon atmosphere. After evaporation, the residue was dissolved in $CHCl_3$ (20 mL) and the organic layer was washed with brine (20 mL). The aqueous layer was further extracted with $CHCl_3$ (2 × 20 mL). The combined organic layer was dried over $MgSO_4$ and evaporated. The residue was purified by flash chromatography (hexane–EtOAc, 1:2) to give **9** as a pale yellow solid (220 mg, 50%). ^{1}H NMR (500 MHz, $CDCl_3$): δ 1.39 (s, 18H), 1.67 (m, 4H), 2.12 (m, 2H), 3.20 (t, 4H, $J = 6.5$ Hz), 3.30 (t, 4H, $J = 6.3$ Hz), 3.62 (m, 2H), 4.09 (t, 2H, $J = 6.0$ Hz), 4.52 (s, 4H), 6.59 (brs, 1H), 6.87 (s, 2H), 6.93 (s, 2H), 7.12 (s, 2H), 7.56 (s, 1H), 7.66 (dd, 2H, $J = 7.5$, 2.0 Hz), 7.69–7.75 (m, 4H), 8.04 (dd, 2H, $J = 7.5$, 2.0 Hz), 8.08 (dd, 1H, $J = 7.9$, 1.4 Hz), 8.16 (d, 1H, $J = 7.9$ Hz). ^{13}C NMR (126 MHz, $CDCl_3$): δ 27.1, 28.1, 28.6, 29.7, 37.8, 39.4, 44.5, 53.5, 66.2, 67.1, 109.5, 112.8, 116.7, 122.6, 122.9, 124.3, 126.3, 127.7, 128.9, 129.5, 130.7, 131.7, 133.1, 133.7, 141.7, 148.2, 149.0, 149.6, 152.6, 157.1, 165.7, 166.5, 167.7, 175.6. HRMS (FAB): m/z calcd for $C_{59}H_{59}N_6O_{18}{}^{35}Cl_2S_2$ $[M + H]^+$ 1273.2704, found 1273.2716; calcd for $C_{59}H_{59}N_6O_{18}{}^{35}Cl_1{}^{37}Cl_1S_2$ $[M + H]^+$ 1275.2675, found 1275.2670.

L^{O}DCF. A solution of KOH (670 mg, 12 mmol) in H_2O (2 mL) was added to a solution of PhSH (125 mL, 1.23 mmol) in CH_3CN (5 mL) at 0 °C under argon atmosphere. After stirring for 30 min, a solution of **9** (520 mg, 0.41 mmol) in CH_3CN (5 mL) was added to the reaction mixture and the resulting solution was further stirred overnight at 50 °C. The mixture was neutralized with 1 M HCl and the solvent was removed by evaporation. The residue was purified by reversed-phase chromatography on an ODS column (H_2O/CH_3CN containing 0.1% TFA 70:30 → 10:90) to give a TFA salt of

L^ODCF as an orange solid (270 mg, 81%). ^{1}H NMR (500 MHz, CD_3OD): δ 1.96–2.03 (m, 6H), 3.26 (t, 4H, $J = 5.8$ Hz), 3.41 (t, 2H, $J = 6.4$ Hz), 3.70 (t, 4H, $J = 5.5$ Hz), 4.06 (t, 2H, $J = 6.1$ Hz), 4.31 (s, 4H), 6.59 (s, 2H), 6.81 (s, 2H), 6.91 (s, 2H), 7.58 (s, 1H), 8.04 (d, 1H, $J = 7.9$ Hz), 8.10 (d, 1H, $J = 7.9$ Hz); ^{13}C NMR (126 MHz, CD_3OD): δ 18.3, 27.3, 29.7, 37.9, 47.0, 50.9, 58.3, 67.8, 69.2, 105.0, 110.2, 112.1, 119.0, 124.3, 127.0, 127.0, 129.3, 129.6, 130.1, 130.9, 131.5, 142.5, 152.6, 153.3, 168.2, 168.7, 169.7; HRMS (FAB): m/z calcd for $C_{37}H_{37}N_4O_8{}^{35}Cl_1{}^{37}Cl_1$ $[M + H]^+$ 737.1959, found 737.1965.

NiL^ODCF. To a mixture of ligand L^ODCF (45.3 mg, 62 μmol) and Et_3N (28 μL, 0.2 mmol) in MeOH (8 mL) was added $Ni(ClO_4)_2 \cdot 6H_2O$ (25.7 mg, 70 μmol) in MeOH (2 mL). After removal of the solvent, the residue was purified by reversed-phase chromatography on an ODS column (H_2O/MeOH 50:50 → 10:90) to give NiL^ODCF as a red-orange solid (40 mg, 81%). MALDI-TOF (pos.): m/z calcd for $C_{37}H_{35}N_4O_8Cl_2Ni_1$ $[M + H]^+$ 791.12, found 791.17; HRMS (FAB): m/z calcd for $C_{37}H_{35}N_4O_8{}^{35}Cl_2Ni_1$ $[M + H]^+$ 791.1185, found 791.1196.

[Ni(L^O)(bpy)](ClO_4)$_2$. A solution of [Ni(L^O)(CH_3CN)$_2$](ClO_4)$_2$[34] (101 mg, 0.18 mmol) and 2,2′-bipyridyl (42 mg, 0.27 mmol) in CH_3CN (1 mL) was stirred for 15 min at room temperature, the mixture was poured into 50 mL of Et_2O. The precipitation thus generated was collected and recrystallized from CH_3CN/Et_2O to give [Ni(L^O)(bpy)](ClO_4)$_2$ as blue crystals (104 mg, 92%). Anal. Calcd for $C_{23}H_{29}N_5O_9Cl_2Ni$: C, 42.56; H, 4.50; N, 10.79%. Found: C, 42.34; H, 4.32; N, 10.89%.

Steady-State Absorption and Fluorescence Spectroscopy. The UV absorption spectra were recorded on a Hewlett-Packard 8453 spectrometer. Fluorescence spectra were recorded using a Hitachi F-2500 spectrometer with a slit width of 2.5 nm. The photomultiplier voltage was 400 V. To reduce the fluctuation in the excitation intensity during measurement, the lamp was kept on for 1 h prior to the experiment. The path length was 1 cm with a cell volume of 3.0 mL. Quantum yields were determined by using fluorescein in 0.1 M NaOH ($\Phi = 0.95$) as the fluorescence standard.[38]

Determination of Apparent Dissociation Constant. The dissociation constant (K_d) of the ternary complex between NiL^ODCF and H6Y1 was determined by fluorescence spectroscopy. A series of HEPES-buffered solutions (50 mM, pH 7.20) of 1.0 μM NiL^ODCF containing various concentrations of H6Y1 peptide ([H6Y1] = 0, 1.4, 4.1, 6.9, 9.6, 13.7, 20.5, 27.2, 40.4, 53.3, and 126.1 μM) were prepared. The sample solutions were stirred for 3 h at room temperature to reach equilibrium and the fluorescence spectra were measured. The subtracted fluorescent intensities at 528 nm ($\Delta F_{528} = F - F_0$, where F_0 means the initial fluorescence intensity) were plotted against the concentrations of H6Y1 and the experimental data were analyzed by nonlinear least square curve fitting using the following equation:

$$\Delta F_{528} = \Delta F_\infty \times \frac{[\mathrm{Ni}]_0 + [\mathrm{H6Y1}] + K_d - \sqrt{([\mathrm{Ni}]_0 + [\mathrm{H6Y1}] + K_d)^2 - 4[\mathrm{Ni}]_0[\mathrm{H6Y1}]}}{2[\mathrm{Ni}]_0} \quad (1)$$

in which ΔF_∞ represents the difference between the initial (F_0) and final (F_∞) fluorescence intensities, and $[Ni]_0$ means the total concentration of NiL^ODCF, that is 1.0 μM.

X-ray Diffraction Data Collection and Determination of Structure. A single crystal was mounted on a CryoLoop (Hamptom Research Co.). Data of X-ray diffraction were collected by a Rigaku RAXIS-RAPID imaging plate two-dimensional area detector with graphite monochromated Mo Kα radiation ($\lambda = 0.71075$ Å) to $2\theta_{max}$ of 55.0°. All data were corrected for Lorentz and polarization effects. All the crystallographic calculations were performed by using a crystal structure software package of the Rigaku Corporation (CrystalStructure version 3.8.2).[39] The crystal structure was solved by direct methods and refined by full-matrix least squares using SIR-92.[40] All hydrogen atoms were refined using the riding model. Crystallographic data have been deposited with Cambridge Crystallographic Data Centre: Deposition number for [Ni(L^O)(bpy)](ClO_4)$_2$ is CCDC-795728. Copies of the data can be obtained free of charge via http://www.ccdc.cam.ac.uk/conts/retrieving.html (or from the Cambridge Crystallographic Data Centre, 12, Union Road, Cambridge, CB2 1EZ, U.K.; Fax: +44 1223 336033; e-mail: deposit@ccdc.cam.ac.uk).

Results and Discussion

Selection of Nickel(II) Complex for the Probe. We attributed the lower binding affinity of Ni–NTA for anionic compounds to electrostatic repulsion, namely the anionic character of the Ni–NTA complex itself. If a DCF fluorophore, which has a net charge of −2 at pH 7, is utilized for the probe based on the fluorophore displacement mechanism, then the corresponding nickel(II) complex requires the following features: (1) a cationic character, which allows the dye to interact with the nickel(II) center, resulting in efficient fluorescence quenching, (2) less steric hindrance around the metal center for facile accessibility of DCF and the His-tag sequence, and (3) comparable binding affinity for the His-tag motif as Ni–NTA complexes.

We have previously reported structural and physicochemical properties of a nickel(II) complex supported by a pyridine-containing macrocyclic tetradentate ligand L^O (=7-oxa-3,11,17-triazabicyclo[11.3.1]heptadeca-1(17),13,15-triene), [Ni(L^O)(X)$_2$]$^{2+}$.[34] In that paper, we mentioned that the affinity of the coordinating solvent molecules (X) located at the apical positions is significantly stronger, and the stable octahedral high-spin nickel(II) is given both in the solid state and in solution. We expected that the core structure of this nickel(II) complex (NiL^O, Figure 1) would be applicable as a fluorescence quencher of DCF as well as a novel interacting partner of the polyhistidine sequence. When NiL^O is conjugated to the DCF dye through a flexible linker, the internal Ni^{II}–DCF complex would be formed and the fluorescence would be quenched. In the presence of His-tagged proteins, on the other hand, the folded structure is expanded by coordinating the histidine imidazoles of the His-tag, and the enhanced emission of DCF can be observed.

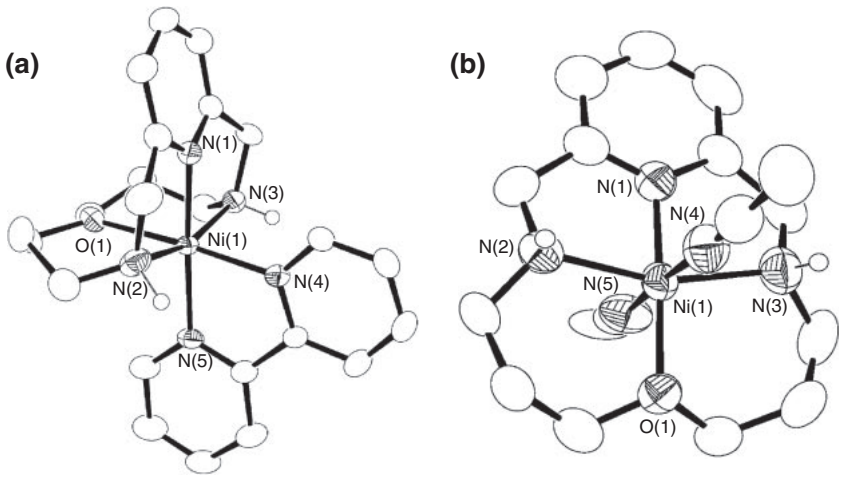

Figure 2. (a) ORTEP drawing of $[Ni(L^O)(bpy)](ClO_4)_2$ showing 50% thermal ellipsoids and selected atom labels. The counter anions and the hydrogen atoms except on nitrogen atoms are omitted for clarity. Selected bond lengths (Å) and angles (deg) for $[Ni(L^O)(bipy)](ClO_4)_2$: Ni(1)–N(1) = 1.9849(18), Ni(1)–N(2) = 2.1032(18), Ni(1)–N(3) = 2.1134(16), Ni(1)–N(4) = 2.0543(18), Ni(1)–N(5) = 2.0636(18), Ni(1)–O(1) = 2.2852(15), N(1)–Ni(1)–N(2) = 81.47(7), N(1)–Ni(1)–N(3) = 81.38(7), N(1)–Ni(1)–N(4) = 97.17(7), N(1)–Ni(1)–N(5) = 176.71(7), N(2)–Ni(1)–N(3) = 162.79(7), N(4)–Ni(1)–N(5) = 79.54(7), N(1)–Ni(1)–O(1) = 89.52(6). (b) Reported crystal structure of $[Ni(L^O)(CH_3CN)_2](ClO_4)(BPh_4)$ (Ref. 32).

Table 1. X-ray Crystallographic Data for $[Ni(L^O)(bpy)](ClO_4)_2$

Empirical formula	$C_{23}H_{29}O_9N_5NiCl_2$
Formula weight	649.12
Crystal size/mm^3	0.30 × 0.10 × 0.10
Crystal system	Monoclinic
Space group	$P2_1/c$ (#14)
a/Å	11.7741(11)
b/Å	16.1901(12)
c/Å	14.2419(13)
β/deg	93.541(3)
V/Å^3	2709.7(3)
Z	4
T/K	133
D_{calcd}/g cm^{-3}	1.591
μ (Mo Kα)/cm^{-1}	9.739
F(000)	1344.00
Total reflections	26687
Unique reflections (R_{int})	6181 (0.050)
Refln./param. ratio	44.15
R_1[a] ($I > 2.00\sigma(I)$)	0.0596
wR_2[b] ($I > 2.00\sigma(I)$)	0.1641
GOF on F^2	1.003

a) $R = \Sigma||F_o| - |F_c||/\Sigma|F_o|$. b) $wR_2 = [\Sigma\{w(F_o^2 - F_c^2)^2\}/\Sigma w(F_o^2)^2]^{1/2}$.

Structural Studies with a Model Ligand. To investigate the structural features of the ternary complex between the NiL^O moiety and the His-tag, we employed 2,2′-bipyridyl (bpy) as the model compound of polyhistidine, which can coordinate to the Ni^{II} center in a bidentate fashion, as found in the Ni–NTA/His-tag pair.[21] Suitable crystals of the nickel(II) complex for X-ray analysis were obtained by vapor diffusion of ether into an acetonitrile solution of $[Ni(L^O)(bpy)]^{2+}$. The crystal data and the experimental parameters are given in Table 1. As shown in Figure 2a, the nickel(II) complex $[Ni(L^O)(bpy)](ClO_4)_2$ is in a distorted octahedral geometry defined by N_3O_1 donor atoms of the macrocyclic ligand L^O and two pyridine nitrogen atoms of the external bpy ligand. No solvent molecule is present in the crystal. Interestingly, the ether oxygen atom of L^O is located perpendicular to the pseudo-plane defined by the metal ion, the pyridine ring, and two secondary amine nitrogens (N1–Ni–O1: 89.52(6)°). The other two coordination sites in a relative *cis*-orientation are occupied by one external bpy ligand. The bent configuration of the macrocyclic framework of L^O observed in the bpy-bound form is different from the reported crystal structure of $[Ni(L^O)(CH_3CN)_2]^{2+}$, where the L^O framework is a flat configuration (Figure 2b).[34] These findings indicate that the structure of the nickel(II) complex can vary depending on the nature of the external ligand. Thus, we worked on the assumption that the His-tag-bound form of the NiL^O complex could adopt a similar bent configuration as observed for $[Ni(L^O)(bpy)]^{2+}$ and that the two histidine imidazoles could similarly coordinate in a bidentate fashion.[41]

Design and Synthesis of NiL^ODCF. We decided to substitute the 4-position of the pyridine ring to link with the DCF dye, because the pyridine substitution would not interfere with the coordination of the His-tag sequence to the Ni^{II} ion. The synthetic scheme of NiL^ODCF is outlined in Scheme 1. The reaction of chelidamic acid diethyl ester with Z-protected propylamine and the following reduction with $NaBH_4$ afforded diol **2**. Pyridine-containing 14-membered macrocyclic ligands are usually synthesized by a one-pot template condensation reaction using 2,6-pyridinedicarbaldehyde, 4-X-1,7-heptanediamine (X = aza, thia, and oxa), and a metal ion such as copper(II) and nickel(II).[34,42] However, these attempts at using 4-substituted 2,6-pyridinedicarbaldehyde were unsuccessful. Instead, synthesis of the macrocyclic unit **6** was achieved by slowly adding dibromide **4** to a solution of nosyl (Ns)-protected diamine **5** in DMF at room temperature. After Z was removed to give **7**, a reaction with an NHS-activated ester of pivaloyl (Piv)-protected fluorescein derivative **8** was performed to afford the fully protected compound **9**. Finally, deprotection

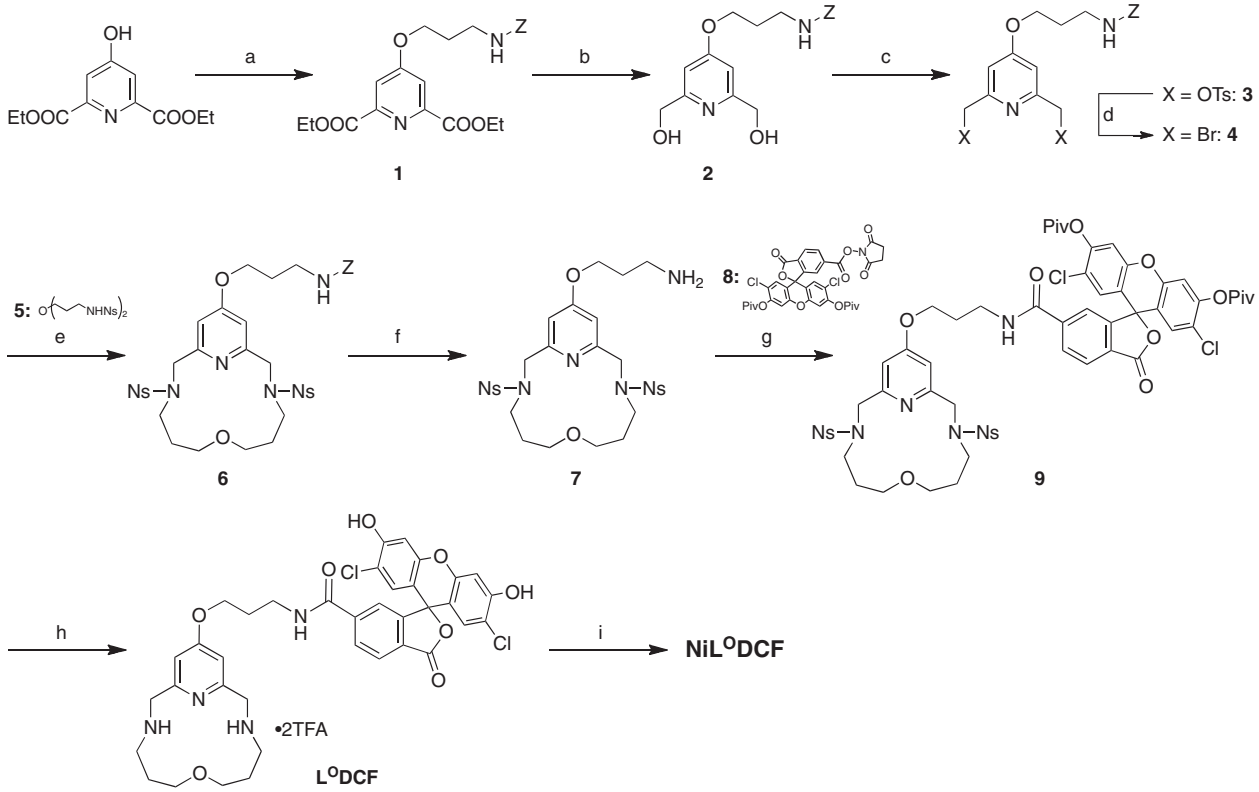

Scheme 1. (a) Benzyl 3-bromopropylcarbamate, K_2CO_3, CH_3CN, reflux, overnight, 62%; (b) $NaBH_4$, EtOH, THF, rt, 1 h, 93%; (c) TsCl, NaOH, water, THF, rt, 4 h, 77%; (d) LiBr, acetone, reflux, 8 h, 100%; (e) **5**, Na_2CO_3, DMF, rt, overnight, 52%; (f) 25%HBr/AcOH, rt, 1 h, 100%; (g) **8**, DMF, rt, overnight, 50%; (h) KOH, PhSH, CH_3CN/H_2O, 50 °C, overnight, then 1 M HCl, 81%; (i) Et_3N, $Ni(ClO_4)_2 \cdot 6H_2O$, MeOH, 81%.

of Ns and Piv groups gave the desired fluorescein-macrocyclic ligand L^ODCF, which was purified by preparative reverse-phase HPLC eluted by H_2O/CH_3CN containing 0.1% trifluoroacetic acid (TFA). Because L^ODCF was isolated as a TFA salt, it was neutralized with NaOH prior to preparation of the nickel(II) complex. Isolation with reverse-phase LC eluted by H_2O/MeOH and following lyophilization afforded desired complex NiL^ODCF as a red-orange powder. It is advantageous for fluorescence labeling experiments that this probe can be used without Ni-complexation, unlike in the case for fluorescent NTA compounds, which need an additional complexation step with the metal ion to label the proteins.[23,24]

Spectroscopic Characterization. All spectroscopic measurements were performed in aqueous buffer solution (50 mM HEPES, pH 7.20). Figure 3 shows the absorption spectra of L^ODCF and NiL^ODCF, where a characteristic band of L^ODCF shifted from 509 ($\varepsilon = 48300\ M^{-1}\,cm^{-1}$) to 488 nm ($\varepsilon = 44300\ M^{-1}\,cm^{-1}$) upon complexation with a nickel ion. Such a hypochromic shift ($\Delta = 21$ nm) in the absorption wavelength indicated that the electronic structure (π-system) of the xanthene core was perturbed in the nickel complex;[43] namely, the phenolic oxygen atom of DCF, rather than the carboxy group at the 2-position of the benzene ring, was directly coordinated to the nickel center in the aqueous buffered solution. The optimized structure of NiL^ODCF by a DFT calculation at the B3LYP/LANL2DZ level also provided the possibility of an interaction between the phenolate oxygen of DCF and the NiL^O moiety (Figure S1 in Supporting Information). It should be noted that the hypochromic shift as shown for NiL^ODCF was not observed for the corresponding cobalt(II) complex of L^ODCF (Figure S2). The fact that there was little change from the original ligand in the absorption spectrum suggested that the fluorescein moiety, in this case, was located from the metal center. The fluorescence of L^ODCF was significantly quenched by complexation with Ni^{II}, as expected

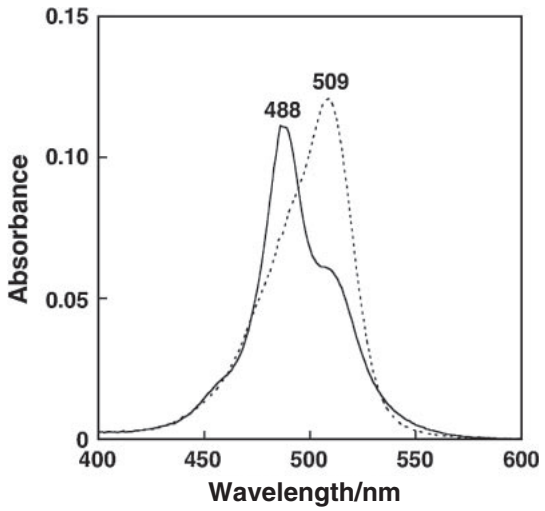

Figure 3. Absorption spectra of L^ODCF (2.5 μM, dashed line) and NiL^ODCF (2.5 μM, solid line) in an aqueous solution (50 mM HEPES, pH 7.20).

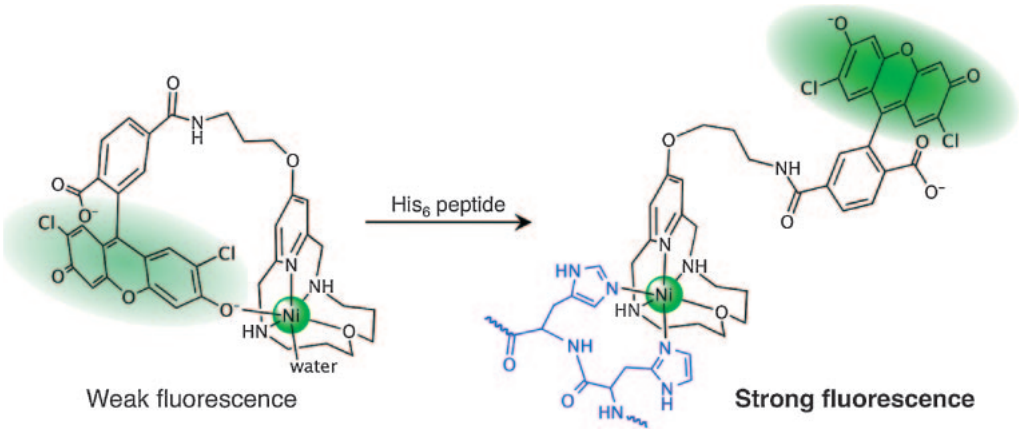

Scheme 2. Displacement of coordinated DCF with histidine imidazoles results in fluorescence enhancement.

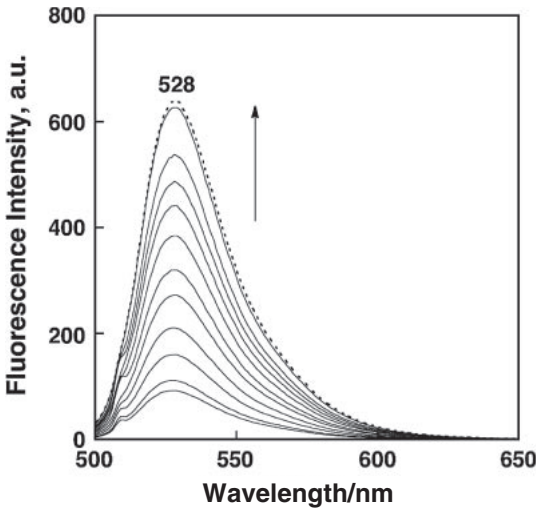

Figure 4. Fluorescence spectral change of NiL^{O}DCF (1.0 μM) upon addition of the hexahistidine peptide (H6Y1). [H6Y1] = 0, 1.4, 4.1, 6.9, 9.6, 13.7, 20.5, 27.2, 40.4, 53.3, and 126.1 μM. The spectra were monitored with an excitation wavelength at 509 nm in 50 mM HEPES buffer (pH 7.20). The dashed spectrum is the macrocyclic ligand L^{O}DCF (1.0 μM) observed under the same conditions.

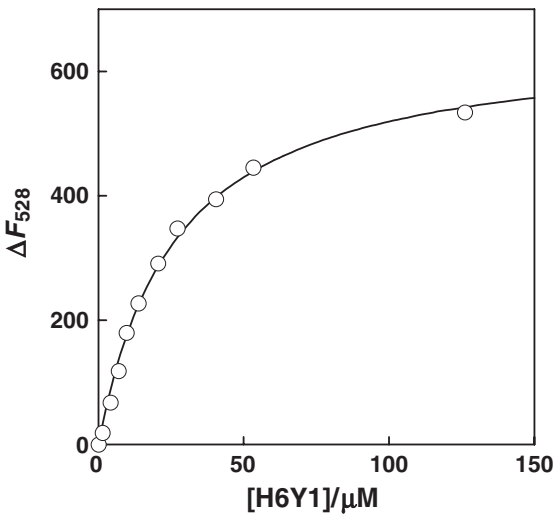

Figure 5. Fluorescence response at 528 nm (λ_{ex} = 509 nm) observed by the titration of NiL^{O}DCF (1.0 μM) with H6Y1 peptide in 50 mM HEPES buffer (pH 7.20). The data were analyzed by nonlinear least-square fitting to determine a dissociation constant of 24 ± 1 μM.

from the absorption data. The quantum yields were 0.60 and 0.084 for L^{O}DCF and NiL^{O}DCF, respectively. These results (86% quenching efficiency) were in contrast to those reported by Lippard et al. showing that the fluorescence of the NTA-functionalized DCF decreased only 5% upon complexation with Ni^{II}.[23] Such a difference in the photochemical properties of DCF was due to the nature of the supporting ligands, L^{O} and NTA. The positively charged NiL^{O} complex coordinated with the DCF dye, as anticipated in the design strategy of the probe.

Fluorescence Response toward His$_6$ Peptide. To model a His-tag-fused protein, we prepared a hexahistidine peptide (H6Y1: YHHHHHH), in which tyrosine was incorporated to determine the accurate concentration of the peptide[24] and evaluated the binding behavior of NiL^{O}DCF by means of fluorescent titration (Scheme 2). The addition of H6Y1 to a 1 μM solution of NiL^{O}DCF resulted in a 7-fold increase in the emission intensity (Figure 4). The fluorescent properties of NiL^{O}DCF were little affected by the presence of biologically relevant ions, such as Na^+, K^+, Mg^{2+}, Ca^{2+}, phosphate (Pi), and pyrophosphate (PPi) (Figure S3), demonstrating that this sensing system will be useful in a wide range of biological and microscopic applications. The intensity of the fluorescence of DCF increased as the concentration of H6Y1 increased, reaching a maximum in the presence of an excess amount of the peptide. The final fluorescent intensity was as high as that observed for the metal-unbound form of L^{O}DCF, indicating no interaction between the DCF fluorophore and the Ni^{II} ion in the H6Y1–NiL^{O}DCF ternary complex. The dissociation of the phenolic oxygen of DCF from the Ni^{II} center in this ternary complex was also confirmed by the absorption spectrum, which showed the disappearance of the characteristic peak at 488 nm attributed to Ni^{II}-bound DCF. The binding stoichiometry of NiL^{O}DCF and H6Y1 was determined to be 1:1 by a Job's plot (Figure S4). Based on this finding, the apparent dissociation constant (K_d) of NiL^{O}DCF for H6Y1 was calculated by the curve fitting analysis of the change of the fluorescence intensity at 528 nm to be 24 μM as shown in Figure 5. This value is

comparable to those reported for Ni–NTA and the hexahistidine peptide ($K_d = 13 \pm 5\,\mu M$),[21–23] suggesting that the two histidine imidazole side chains of the His-tag bind NiL^O core with a manner similar to the case of Ni–NTA. In addition, we performed a labeling experiment of His_6-coated resin beads with NiL^ODCF to evaluate the binding properties of the probe. When the NiL^ODCF-labeled His_6-beads were washed several times with a neutral aqueous buffered solution, a red color remained on the resin, indicating that the probe is still immobilized on the resin surface. In contrast, the probe was easily dissociated from the beads by washing with an EDTA-containing buffer, which is a direct evidence for the Ni-mediated interaction between NiL^ODCF and the His_6 peptide on the resin. Thus, these results suggest that NiL^ODCF undergoes a slow dissociation from the His_6–NiL^ODCF complex and demonstrate the usefulness of NiL^ODCF for optical imaging of specific protein expressed on the cell surface.

Conclusion

We have designed a novel "turn-on" fluorescent probe NiL^ODCF for the His-tag sequence of proteins on the basis of the fluorophore displacement mechanism. We demonstrated that a macrocyclic nickel(II) complex moiety NiL^O incorporated into the probe can act as the fluorescence quencher through a labile coordinative interaction and can serve as the His-tag binding site. NiL^ODCF exhibits an increase in fluorescence in the presence of the His-tag. The 1:1 stoichiometry and dissociation constant (K_d) for the interaction between NiL^ODCF the hexahistidine peptide are comparable to those for the Ni–NTA/His_6 pair. These features for NiL^ODCF, which include the switchable fluorescence response, the reasonable K_d value, and the visible light excitation, would allow fluorescent labeling of the His-tag-fused proteins, as well as optical cell imaging. We consider further applications of NiL^ODCF to fluorescence-based enzyme assay tools in which enzymatic reactions result in an alteration of the binding affinity of the fluorophore, triggering an increase in fluorescence.

This work was financially supported by a Grant-in-Aid for Young Scientists (B) (No. 21750168 to M.T.) and Grant-in-Aid for JSPS Fellows (T.H.).

Supporting Information

DFT optimized structure for NiL^ODCF, UV–vis spectrum of cobalt(II) complex, fluorescence response toward biologically relevant ions, Job's plot, and mass spectra for L^ODCF and NiL^ODCF. This material is available free of charge on the web at http://www.csj.jp/journals/bcsj/.

References

1 J. Zhang, R. E. Campbell, A. Y. Ting, R. Y. Tsien, *Nat. Rev. Mol. Cell Biol.* **2002**, *3*, 906.
2 B. N. G. Giepmans, S. R. Adams, M. H. Ellisman, R. Y. Tsien, *Science* **2006**, *312*, 217.
3 R. Y. Tsien, *Annu. Rev. Biochem.* **1998**, *67*, 509.
4 A. Chiesa, E. Rapizzi, V. Tosello, P. Pinton, M. de Virgilio, K. E. Fogarty, R. Rizzuto, *Biochem. J.* **2001**, *355*, 1.
5 C. S. Lisenbee, S. K. Karnik, R. N. Trelease, *Traffic* **2003**, *4*, 491.
6 O. Agbulut, A. Huet, N. Niederländer, M. Puceat, P. Menasché, C. Coirault, *J. Biol. Chem.* **2007**, *282*, 10465.
7 M. Fernández-Suárez, A. Y. Ting, *Nat. Rev. Mol. Cell Biol.* **2008**, *9*, 929.
8 E. M. Sletten, C. R. Bertozzi, *Angew. Chem., Int. Ed.* **2009**, *48*, 6974.
9 N. Soh, *Sensors* **2008**, *8*, 1004.
10 B. A. Griffin, S. R. Adams, R. Y. Tsien, *Science* **1998**, *281*, 269.
11 A. Keppler, S. Gendreizig, T. Gronemeyer, H. Pick, H. Vogel, K. Johnsson, *Nat. Biotechnol.* **2003**, *21*, 86.
12 I. Chen, M. Howarth, W. Y. Lin, A. Y. Ting, *Nat. Methods* **2005**, *2*, 99.
13 C.-W. Lin, A. Y. Ting, *J. Am. Chem. Soc.* **2006**, *128*, 4542.
14 A. Ojida, K. Honda, D. Shinmi, S. Kiyonaka, Y. Mori, I. Hamachi, *J. Am. Chem. Soc.* **2006**, *128*, 10452.
15 C. T. Hauser, R. Y. Tsien, *Proc. Natl. Acad. Sci. U.S.A.* **2007**, *104*, 3693.
16 G. V. Los, L. P. Encell, M. G. McDougall, D. D. Hartzell, N. Karassina, C. Zimprich, M. G. Wood, R. Learish, R. F. Ohane, M. Urh, D. Simpson, J. Mendez, K. Zimmerman, P. Otto, G. Vidugiris, J. Zhu, A. Darzins, D. H. Klaubert, R. F. Bulleit, K. V. Wood, *ACS Chem. Biol.* **2008**, *3*, 373.
17 A. Ojida, S. Fujishima, K. Honda, H. Nonaka, S. Uchinomiya, I. Hamachi, *Chem. Asian J.* **2010**, *5*, 877.
18 K. Honda, E. Nakata, A. Ojida, I. Hamachi, *Chem. Commun.* **2006**, 4024.
19 D. L. Johnson, L. L. Martin, *J. Am. Chem. Soc.* **2005**, *127*, 2018.
20 A. N. Kapanidis, Y. W. Ebright, R. H. Ebright, *J. Am. Chem. Soc.* **2001**, *123*, 12123.
21 S. Lata, A. Reichel, R. Brock, R. Tampé, J. Piehler, *J. Am. Chem. Soc.* **2005**, *127*, 10205.
22 E. G. Guignet, R. Hovius, H. Vogel, *Nat. Biotechnol.* **2004**, *22*, 440.
23 C. R. Goldsmith, J. Jaworski, M. Sheng, S. J. Lippard, *J. Am. Chem. Soc.* **2006**, *128*, 418.
24 M. Kamoto, N. Umezawa, N. Kato, T. Higuchi, *Chem.—Eur. J.* **2008**, *14*, 8004.
25 M. Kamoto, N. Umezawa, N. Kato, T. Higuchi, *Bioorg. Med. Chem. Lett.* **2009**, *19*, 2285.
26 N. Soh, D. Seto, K. Nakano, T. Imato, *Mol. BioSyst.* **2006**, *2*, 128.
27 L. Fabbrizzi, M. Licchelli, P. Pallavicini, L. Parodi, *Angew. Chem., Int. Ed.* **1998**, *37*, 800.
28 K. J. Franz, N. Singh, S. J. Lippard, *Angew. Chem., Int. Ed.* **2000**, *39*, 2120.
29 S. C. Burdette, G. K. Walkup, B. Spingler, R. Y. Tsien, S. J. Lippard, *J. Am. Chem. Soc.* **2001**, *123*, 7831.
30 T. Hirano, K. Kikuchi, Y. Urano, T. Nagano, *J. Am. Chem. Soc.* **2002**, *124*, 6555.
31 L. Zeng, E. W. Miller, A. Pralle, E. Y. Isacoff, C. J. Chang, *J. Am. Chem. Soc.* **2006**, *128*, 10.
32 Y. Urano, D. Asanuma, Y. Hama, Y. Koyama, T. Barrett, M. Kamiya, T. Nagano, T. Watanabe, A. Hasegawa, P. L. Choyke, H. Kobayashi, *Nat. Med.* **2009**, *15*, 104.
33 G. Sharma, J. P. Tandon, *J. Inorg. Nucl. Chem.* **1970**, *32*, 1273.
34 M. Taki, Y. Kawashima, N. Sakai, T. Hirayama, Y. Yamamoto, *Bull. Chem. Soc. Jpn.* **2008**, *81*, 590.
35 A.-S. Chauvin, S. Comby, B. Song, C. D. B. Vandevyver,

J.-C. G. Bünzli, *Chem.—Eur. J.* **2008**, *14*, 1726.

36 C. C. Woodroofe, R. Masalha, K. R. Barnes, C. J. Frederickson, S. J. Lippard, *Chem. Biol.* **2004**, *11*, 1659.

37 T. Hirayama, M. Taki, A. Kodan, H. Kato, Y. Yamamoto, *Chem. Commun.* **2009**, 3196.

38 J. R. Lakowicz, *Principles of Fluorescence Spectroscopy*, 3rd ed., Springer, New York, **2006**.

39 *CrystalStructure 3.8.2: Crystal Structure Analysis Package*, Rigaku and Rigaku/MSC, The Woodlands, TX 77381, USA, **2007**.

40 SIR92: A. Altomare, G. Cascarano, C. Giacovazzo, A. Guagliardi, M. C. Burla, G. Polidori, M. Camalli, *J. Appl. Crystallogr.* **1994**, *27*, 435.

41 It is also possible that the macrocyclic ligand of NiL^{O} adopts a flat conformation in the His-tag bound form, where two histidine imidazoles occupy both axial positions of the NiN_3O_1 plane, and these bent- and flat-configurations are hardly distinguishable from each other in the spectroscopic properties. However, we considered that for the flat conformation the steric repulsion between the ligand framework and the histidine residues of His-tag would make it less favorable for the tag sequence to adopt a hairpin-like structure.

42 V. Félix, M. J. Calhorda, J. Costa, R. Delgado, C. Brito, M. T. Duarte, T. Arcos, M. G. B. Drew, *J. Chem. Soc., Dalton Trans.* **1996**, 4543.

43 V. Balzani, F. Scandola, *Supramolecular Photochemistry*, Ellis Horwood, New York, **1991**.